Aldol condensation of biomass-derived levulinic acid and furfural over acid zeolites

Jennifer Cueto[1], Valeria Korobka[2], Laura Faba[1], Eva Díaz[1], Salvador Ordóñez[1*]

[1]Catalysis, Reactors and Control Research Group (CRC), Dept. of Chemical and Environmental Engineering, University of Oviedo, Oviedo 33006, Spain

[2]Department of Chemical and Process Engineering, University of Strathclyde, 75 Montrose Street, Glasgow G11XJ, Scotland, UK

*e-mail: sordonez@uniovi.es, Tel: +34 985 103 437; Fax: + 34 985 103 434

ABSTRACT. Acid-catalysed cross condensation between furfural and levulinic acid is presented in this work as an alternative for manufacturing C10 chemicals from renewable platform molecules. First experiments conclude that the neutralization of the carboxylic group of levulinic acid is required to prevent side reactions such as cyclization. Two C10 products are obtained, suggesting two parallel reaction mechanisms. Different reaction conditions (temperatures and initial reactants ratios) have been tested, and results were used to propose a kinetic model. The role of the properties of different catalysts is also studied, analysing the activity, selectivity and acidities of different zeolites structures (ZSM-5, MOR, BETA), observing a clear correspondence between medium-strength acidity and the production of the most stable product. A high selectivity to this compound is required to reduce the permanent adsorption and oligomerization of the starting materials, the main deactivation cause identified in this process. Thus, the best results were obtained with ZSM-5 (23) at 423 K and a LA:FFL ratio 2:1, with 50 % of products yield and almost negligible relevance of side reactions (carbon balance after 24 h: 91 %), observing a good behaviour after three reusability cycles without any regeneration.

KEYWORDS: Biomass upgrading, sodium levulinate, acid catalysis, ZSM-5, C-C coupling, biorefinery.

INTRODUCTION

In the new strategies for replacing petrochemicals by renewable carbon-based chemicals, the difficult for selectively preparing chemicals with carbon chains of more than six carbon atoms is still a huge challenge, since most of the biobased platform molecules have six or less carbon atoms.[1,2] Aldol condensation reactions are considered among the most interesting reactions to produce C-C bonds between these bio-platform molecules.[3-8] Despite the existence of other alternatives (such as Claisen, Knoevenagel, Guerbet condensations, or biological processes, among others),[9-12] aldolization stands out because of the mild reaction conditions used (typically ambient pressure and temperatures below 450 K), and the huge amount of potential raw materials directly obtained from biomass (furfural -FFL-, 5-HMF, acetone, cyclopentanone, etc.), with two alternative coupling mechanisms known (via enol or enolate intermediate, as function of using acid or basic catalysts, respectively).[13-15]

Levulinic acid (LA) is a very interesting bio-platform molecule.[16,17] Several alternative production routes are reported in the literature, the most promising one being the Biofine process and its production via furfuryl alcohol, with final yields higher than 70 % using commercial zeolites.[18,19] LA is proposed as starting compound of many different processes, most of them involving its internal cyclization and the subsequent hydrogenation to γ-valerolactone,[20-23] a reaction in principle known since the 1930's.[24] Typically, the carboxylic group of LA plays a key role in the mechanism, other routes involving the activity of the

carbonyl group being scarcely investigated, as is the case of aldol condensation. This reaction would allow obtaining a family of C10 compounds with promising uses as fuel additives, surfactants, lubricants or pharmaceutical precursors.[25,26]

LA self-condensation has been proposed considering basic and acid materials (mixed oxides, Amberlyst-15, etc.), concluding that results are strongly conditioned by the competition between the activity of the carbonyl group and the carboxyl one.[25-27] Thus, more than 30 % of angelica lactone (C5) is produced at 323 K, with only 40 % LA conversion. The yield of this compound increases with the temperature, being the main limitation of this procedure.[25]

The predominance of cyclization suggests that LA self-condensation is not fast enough to prevail over this undesired side reaction. The cross-condensation approach, involving a more active molecule, is the natural way to continue these studies, with FFL or 5 HMF being good alternatives, successfully tested in similar reactions.[13,28,29] Both cyclic aldehydes are obtained by the hydrolysis and dehydration of sugar polymers.[30,31] Thus, the co-production of both reactants is an additional advantage, reducing the purification steps required. However, LA is obtained by the rehydration of 5-HMF under acidic conditions, so the use of this molecule is not suggested, to avoid interactions related to the decomposition of 5 HMF into LA.[32,33] FFL has been previously proposed as a co-reactant in most of the aldol condensation processes used, obtaining very promising results with different platform molecules.[34-36] Despite its well-known activity, there are only two papers considering LA and FFL condensation. In the first one, NaOH is proposed as catalyst, giving 95 % yield after 48 h reaction time at 273 K.[37] Despite the undoubted relevance of this study as a first approach to the reaction mechanism, the use of

homogeneous catalysis is against of the main Principles of Green Chemistry. Concerning the heterogeneous catalysts, different materials were tested in a preliminary screening in a second study.[38] In general, FFL conversions lower than 40 % were reported, except in the cases where overall selectivities are far from 100 %, suggesting the presence of undesired reactions. In this context, a deep study is required, since the reaction conditions were not optimized, and no references to side reactions, carbon balances or deactivation were included.

The aim of this work is to present the results obtained in the study of FFL and LA cross-condensation using different acid zeolites (widely available acid catalysts). Reactions conditions were optimized, in terms of temperature and initial reactants ratio. The role of acidity as well as structural properties of zeolitic catalysts was also studied. The experimental data were used to propose a kinetic model. Reusability tests were also carried out with reaction conditions previously optimized.

EXPERIMENTAL SECTION

Catalysts and characterization

NH$_4$-ZSM-5 (CBV 2314), NH$_4$-ZSM-5 (CBV 8014), NH$_4$-MOR (CBV 21A) and NH$_4$-BETA (CP 814E) were provided by Zeolyst International. The framework SiO$_2$/Al$_2$O$_3$ ratios were 23, 80, 20 and 25, respectively. These materials have been activated at 823 K for 12 h to transform NH$_4$ functional groups into H-forms.

Acidic properties of these catalysts have been evaluated by two different techniques: titration with NaOH and temperature programmed desorption of NH_3 (NH_3-TPD) using a Micromeritics TPD/TPR 2900. With respect to the first one, 25 mg of each catalyst were introduced into 50 ml of 0.1 M solution of NaCl, acidifying the mixture previously with 0.5 ml of 0.1 M HCl. After 3 h of stirring at room temperature, different volumes of 0.1 M NaOH were added by measuring with each addition the pH until neutral pH was obtained. In addition, a titration of a blank was performed in order to calculate the total acidity by subtracting the volume of NaOH consumed with each catalyst from the corresponding one of the blank. Thus, the meq H^+/g were obtained for each material analysed. Concerning the TPD analyses, NH_3 signal evolution was measured with Pfeiffer Vacuum Omnistar Quadrupole Mass Spectrometer. 20 mg of sample were employed in each analysis. In order to remove any compound physisorbed on the surface, samples were pretreated before each analysis, by heating to 383 K in helium flow (20 ml·min^{-1}) for 1 h. Subsequently, the catalytic surface was saturated in NH_3 flow (2.5 % NH_3/He, 20 ml·min^{-1}) at room temperature for 15 min. An intermediate stage of stabilization under helium flow was required to prevent signals related to oversaturation. Then, the desorption of physisorbed NH_3 was monitored, being flushed with helium (20 ml·min^{-1}) from room temperature to 823 K with a temperature rate of 5 K·min^{-1}.

Morphological properties of the zeolites (surface area, pore diameter and micro- and total pore volumes) were determined by nitrogen physisorption at 77 K using an ASAP 2020 (Micromeritics) static volumetric apparatus after the a degasification step at 383 K during 6 h.

Catalytic performance

LA and FFL aldol condensation was carried out in a 0.5 L stirred batch autoclave reactor equipped with a PID temperature controller and a backpressure regulator (Autoclave Engineers EZE Seal). Firstly, 100 ml of an aqueous solution of LA (2 M, Sigma Aldrich, 99%) was neutralized with a 0.1 mol of Na_2CO_3 (Panreac, 99 %) obtaining the corresponding salt (sodium levulinate, labelled as NaLe). The reactor was loaded with 0.25 L of an aqueous solution of FFL (Sigma Aldrich, 99%) and NaLe solution (5 % wt. of reactants) and 1.8 g of zeolite (50-80 μm). Different reactants ratios were considered, the specific values being detailed in each corresponding reaction. Considering that a blank experiment allows discounting the self-catalytic reaction, the feed was pre-heated to 343 K before the catalyst was introduced. Thus, the starting point is better defined, minimizing mistakes related to reaction evolution before reaching the desired temperature. The analysis of reaction mixture at initial time discounts any decomposition or undesired reaction of any reactants. Different reaction temperatures were studied, from 323 to 448 K, the particular value being indicated in each analysis. Before starting the reaction, the reactor is purged with nitrogen, and the reaction is carried out under 15 bar of N_2 with a stirring of 1000 rpm for 24 h. Operation pressure was selected for both ensuring the absence of water or furfural evaporation at any working conditions, since their boiling points (373 K and 434 K, respectively) are lower than the maximum temperature tested; and guaranteeing an excess enough to take the samples from the sampling point under safety conditions, (a overpressure is required to pump the liquid) without producing a relevant decrease in the reactor pressure that can favors the evaporation of any compound after taking several samples.

Samples were taken from the reactor to obtain the evolution of reactants and products

concentration during the reaction. A filter was placed in the sample port in order to prevent the

extraction of catalyst and possible solids, which had formed during the reaction. The samples

were extracted with ethyl acetate (volume ratio of 1:1) and acidified with HCl (2:1 volume ratio

aqueous phase: solution 1 M of HCl). The organic phase was analysed by GC in a Shimadzu GC-

2010 equipped with a FID detector, using a 30 m long CP-Sil 8 CB capillary column. Peak

assignment was carried out by GC-MS in a Shimadzu GC/MS QP 2010 Plus Instrument, using a

30 m long TRB-5MS capillary column. The calibrations of LA and FFL were performed using

authentic samples, whereas the calibration of the products (labelled as δ-C10 and β-C10) was

done using the relative carbon concept proposed by Scanlon and Willis[39] since they are not

commercially available. Catalysis results were described in terms of conversion, atomic yield

and carbon balance closure, being calculated as follows (Equations 1-3):

$$Conversion\ (\%) = 100 \cdot \frac{(reactant_{t=0} - reactant_t)}{reactant_{t=0}} \qquad (1)$$

$$\Psi_{C10}\ (\%) = 100 \cdot \frac{10 \cdot ([\delta - C10] + [\beta - C10])_t}{(5 \cdot [LA] + 5\ [FFL])_{t=0}} \qquad (2)$$

$$C.B.\ (\%) = 100 \cdot \frac{10 \cdot ([\delta - C10] + [\beta - C10])_t + 5 \cdot ([LA] + [FFL])_t}{(5 \cdot [LA] + 5 \cdot [FFL])_{t=0}} \qquad (3)$$

The spent catalysts were recovered by filtration, washed and dried overnight at 373 K before

their analysis by different techniques. TPD analyses were performed to determine possible

adsorption of different compounds on the catalyst's surface. These experiments were carried

out using a Micromeritics TPD/TPR 2900 with a helium flow of 20 ml·min^{-1} increasing the

temperature up to 1273 K with a 5 K·min^{-1} rate. Initial TPDs of fresh catalysts were done to

ensure that materials were stable to the maximum temperature analyzed. The evolution of different signals was measured with a Pfeiffer Vacuum Omnistar Quadrupole Mass Spectrometer. Experimental results were compared to the m/z spectra of all the compounds involved, according to data compiled by NIST Mass Spec Data Centre for reactants and the experimental spectrums obtained by GC-MS technique for products (δ-C10 and β-C10): FFL (m/z = 29, 38, 39, 67, 95, 96); LA (m/z = 43, 56, 73, 101, 116); δ-C10 (65, 93, 121, 148, 177, 194); and β-C10 (77, 78,79, 105, 108, 150, 194). Considering that the mass spectrometer is more sensitive for small m/z values, 39, 43, 65 and 77 were chosen as the signals for the analyses for FFL, LA, δ-C10 and β-C10, respectively. Using the same equipment and procedure, but introducing an oxidizing atmosphere (20 ml·min^{-1} of 2 % O_2 in He), TPO (temperature-programmed oxidation) tests were carried out to compare different carbonaceous deposits on catalyst surfaces by monitoring the CO_2 release.

RESULTS AND DISCUSION

Reaction mechanism and kinetic model

Considering our previous results with LA self-condensation,[25] a Mg-Zr mixed oxide catalyst was proposed as a first approach to LA and FFL cross-condensation. The reaction was carried out at 323 K, with equimolar initial reactants ratio and a catalytic loading of 0.5 g. No C10 compounds were detected but a large amount of angelica lactone was formed (final yield of 12 % with LA conversion of 21 % after 24 h). This reaction has been previously reported in the literature.[40] This result suggests that internal LA cyclization prevails over cross-condensation, i.e., the

homogeneous catalysis by the low pH of a levulinic acid solution (pH = 2.5) prevails over the activity of the solid catalyst. According to this, the carboxylic acid functional group must be neutralized to prevent this undesired process. In addition, the carbon balance strongly decreases (54 %) being explained by the strong interaction between FFL (and LA at a lesser extent) and medium strength basic-acid pairs of Mg-Zr mixed oxide. This interaction enhances the permanent adsorption, causing oligomerization to solids blocking the active sites.

Based on these conclusions, the basic catalysis is abandoned, focusing the study on the activity of acid catalysts, such as ZSM-5 zeolite. This material has been widely proposed as catalyst for different biomass upgrading reactions,[41,42] highlighting its activity in reactions requiring strong acidity.[43,44] To prevent the competence between the carboxylic group of LA and the carbonyl one (promoting undesired reactions such as cyclization), a previous esterification with ethanol was considered, studying the reaction between ethyl levulinate (EL) and FFL. Ethanol is chosen due to its renewable origin and non-hazard character, trying to respect the Principles of Green Chemistry. No conversions are observed when working at 323 K and 0.5 g of ZSM 5. The reaction temperature was then increased up to 373 K, but no C10 compounds are detected even at these conditions. By contrast, LA is obtained (7 % as yield after 24 h), suggesting that esterification is partially reversible at these conditions. This equilibrium has been previously proposed in the literature.[45] The negligible formation of angelica lactone is congruent with the previous result (higher concentrations of LA are required to obtain a quantifiable cyclization), and the more neutral pH of this configuration (3.5 vs. 2.5 when working with LA). To sum up, using EL as reactant, there is not good balance between the severity of the required reaction

conditions and the stability of the resulting ester. Thus, this was also abandoned for further investigations.

In a third approach, the neutralization with an inorganic salt (Na_2CO_3) is proposed, in order to effect the desired reaction between sodium levulinate (NaLe) and FFL. In this approach, the use of the salt requires a subsequent acidification of products obtained, using HCl (details given in the Experimental section). Despite this procedure may challenge the sustainability of this process, both reactants were chosen considering the required neutralization with the lowest hazard level of wastes generated (NaCl).

The evolution of reactants conversion and products yields, as well as the carbon balance closure is shown in **Figure 1**. The reaction is carried out at 373 K and using 1.8 g of ZSM 5 (23) and equimolar ratio of both reactants. Negligible reactant conversions were observed at lower temperatures.
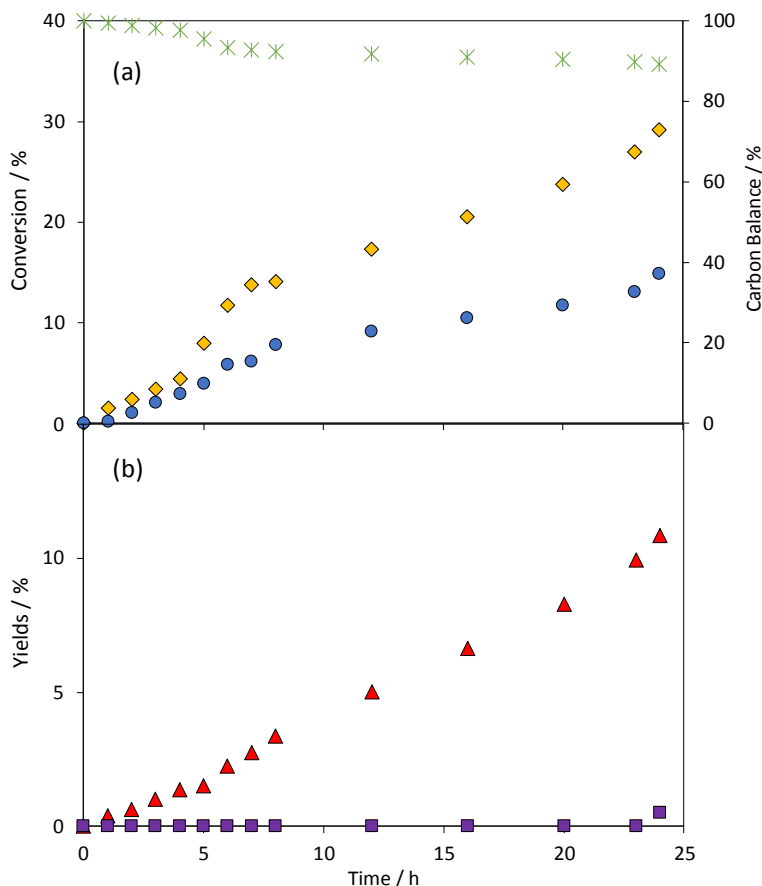
Figure 1. Temporal evolution of (a) reactants conversions and (b) product yields. Results corresponding to NaLe-FFL aldol condensation at 373 K, using 1.8 g of ZSM-5 (23) and equimolar reactant ratio. Symbols: (●) NaLe; (♦) FFL; (✻) carbon balance; (▲) β-C10; (■) δ-C10.

The highest FFL conversion observed (29.2 % after 24 h) in comparison to the14.9 % obtained

with NaLe (this conversion could directly referred to the levulinic acid one since the GC analysis

is carried out once it was acidified with HCl, the LA being the compound quantified), as well as

the lack of correspondence with the products total yield (11.3 %) suggest the permanent

adsorption or even oligomerization of FFL on the catalyst's surface. This hypothesis is congruent

with the carbon balance, showing a progressive decrease to 89.2 % after 24 h. As to the

products analysis (once, four main peaks were detected. According to the m/z spectra obtained

by GC-MS (shown in Figure S1), they can be grouped in two different C10 products: a branched compound labelled as β-C10 (main product, with a final yield of 10.8 %); and a linear one, δ-C10 (0.5 % final yield). Each compound has two isomers (cis and trans), considered together in the analysis. Globally, the reaction mechanism suggested by the experimental results is summarized in **Scheme 1**.
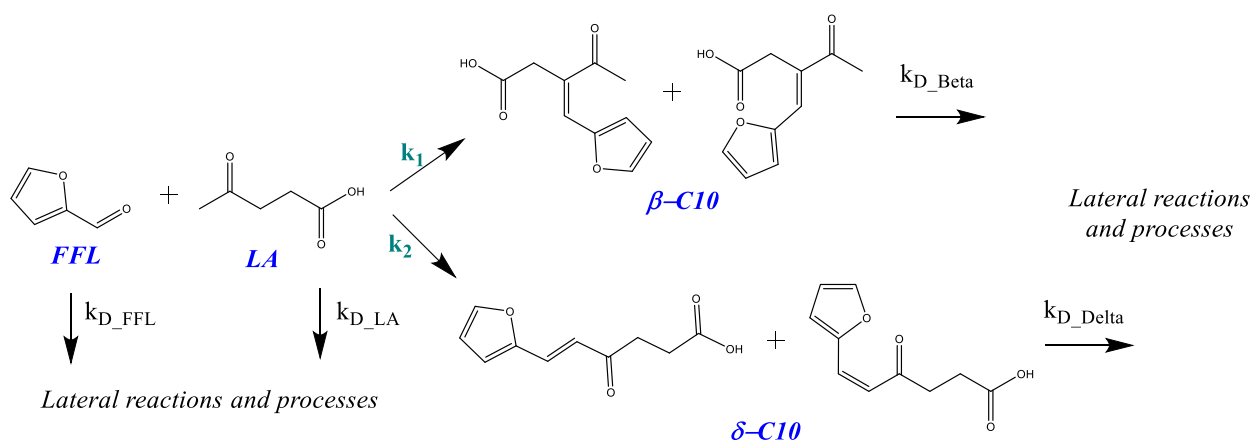
Scheme 1. Proposed reaction network for FFL-LA aldol condensation.

According to these results, the general acid aldolization mechanism is divided into two reaction pathways, as function of the site of proton abstraction, either on the tertiary carbon (producing the branched compound, β-C10), or on the terminal carbon. In this latter case, the linear product is obtained. These divergent routes are detailed in **Scheme 2**. The first step of this mechanism is the protonation of the carbonyl group of NaLe, by the interaction with the proton of the hydroxyl group present on the catalyst surface.[46] The protonated species then undergo tautomerization, producing the subsequent enol. Two different compounds can be obtained, since the nucleophilic attack can concern two different α proton of the levulinate. Successively,

these enols attack the carbonyl group of FFL, producing a β-hydroxy ketone (C10-OH). This intermediate is not observed because it undergoes fast dehydration, yielding the α-β-unsaturated ketones (β- and δ-C10). Since terminal enols are less stable, selectivity to the β -isomer is largely higher than the corresponding to δ -isomer.
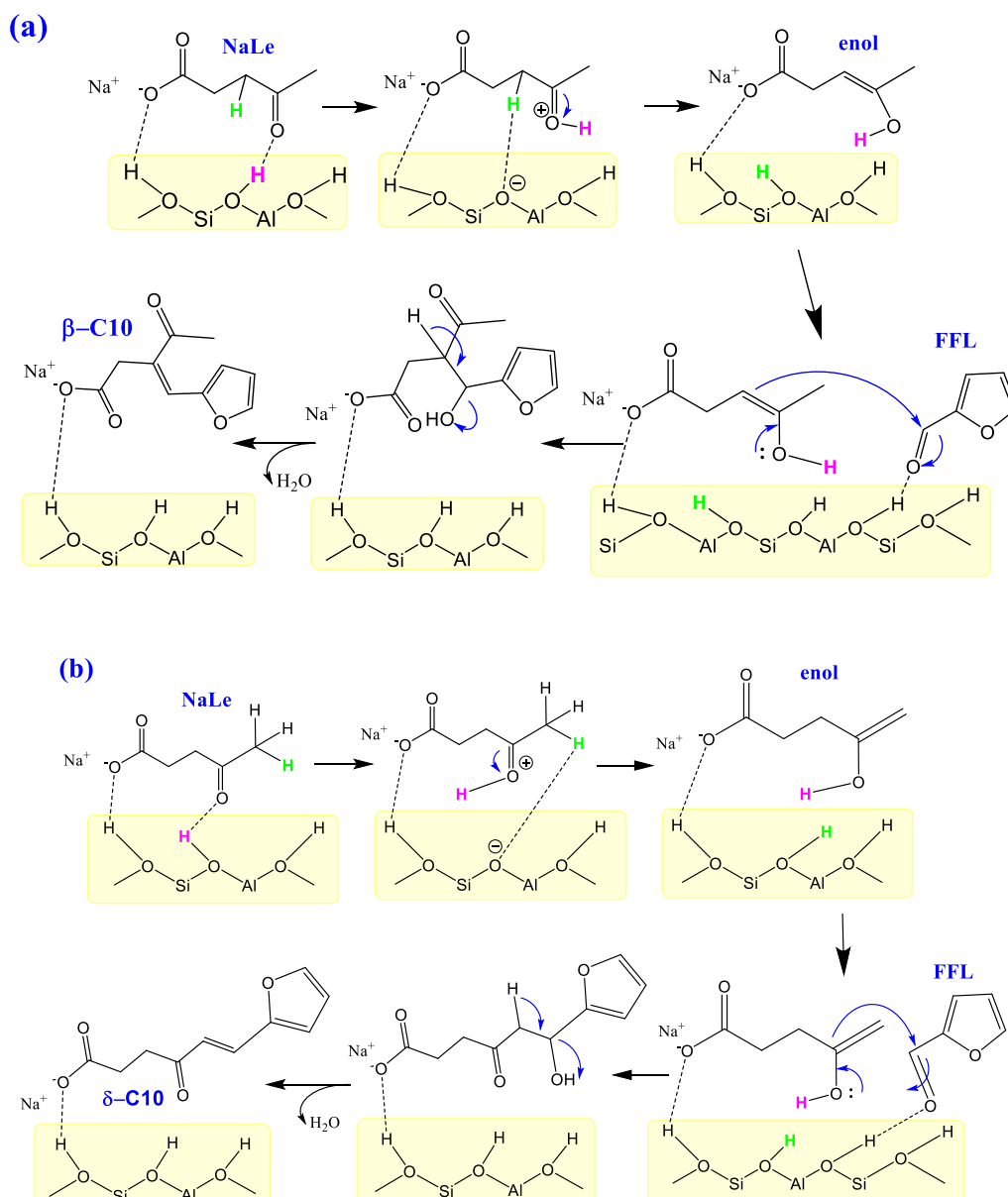


Scheme 2. Reaction mechanism of NaLe-FFL aldol condensation catalysed by acid zeolites to obtain (a) β-C10 and (b) δ-C10.

None of these steps directly involves the carboxylic group. Therefore, it is not evident why the reaction takes place when working with the NaLe but not with LA or EL. In aqueous medium, NaLe is totally dissociated into Na^+ and levulinate. As the reaction pH (6) is higher than the pKa of the LA (4.64), anion prevails over the protonated form, when the NaLe is used as reactant. In the case of LA, the situation is the opposite: as the pH of the reaction (pH=2.57) is lower than the pKa (4.64), so most of the levulinate is presented in its protonated form. We assume that the interaction between levulinate or levulinic acid and the catalytic surface is the key parameter in this discussion. Based on these facts, we propose that the adsorption of levulinic acid on the catalyst surface is too weak to initiate the reaction, while the adsorption of levulinate is co-operatively enhanced by the carboxylate anion. In good agreement with this hypothesis, the reaction with EL does not take place, since most of the levulinate obtained by the reverse reaction is directly protonated (pH = 3.5). This hypothesis was tested by comparing the amount of LA and NaLe adsorbed on the ZSM-5. Working at the same initial concentration (0.236 mol·L^{-1}), the amount of levulinate adsorbed on the zeolite is more than 7 times higher than the amount of LA adsorbed (0.9 and 5.7 %, respectively).

Considering the different distribution of both compounds, a predominant production of β-C10 is suggested, in good agreement with the higher stability of anions involving highly substituted carbons. This fact is emphasized by comparing the evolution of β-C10/δ-C10 ratio with the time. This magnitude decreases from infinity at the initial moments (no δ-C10 is quantitatively detected during the first 20 h of reaction) to 21.5 after 24 h. This evolution could be explained by two different or synergetic reasons. On the one hand, if both compounds are obtained on the same acid sites, longer times are required to promote the linear adduct (slower kinetics).

On the other hand, if both products require different acidity strengths, then the first set of active sites are partially blocked during the reaction, enhancing the proportion of free acid sites involved in the formation of the linear compound.

In order to check the first hypothesis, a kinetic analysis had to be carried out, requiring studying the reaction at different temperatures. The influence of this parameter was study by analyzing the experimental results obtained at 393, 423 and 448 K in comparison to the previous results at 373 K, with **Figure 2** comparing the results.
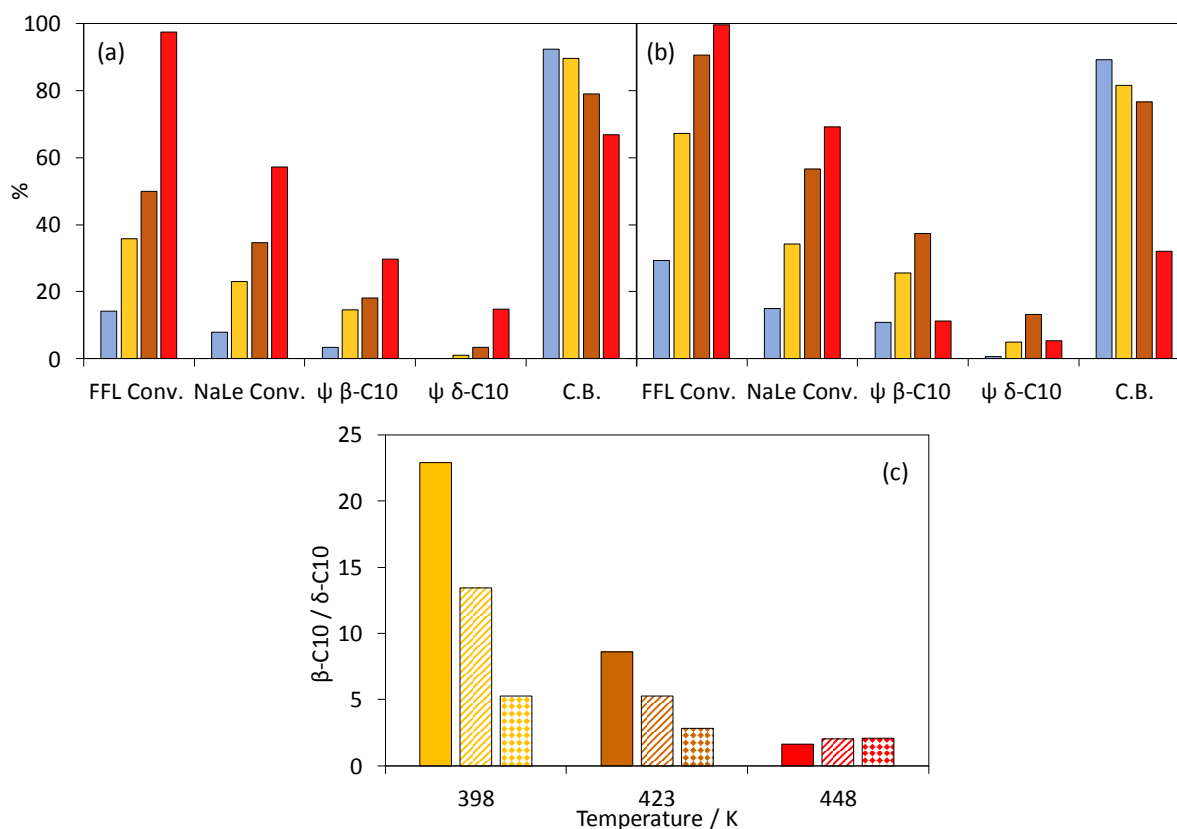
Figure 2. Summary of results obtained of NaLe-FFL aldol condensation catalysed by 1.8 g of ZSM-5 (23) as a function of the temperature and the reaction time (equimolar reactants ratio). Legend: (a) 8 h, (b) 24h and (c) products ratio at different times: 4 h (solid columns), 8 h (dashed columns) and 24 h (diamond columns); 373 K (blue); 398 K (yellow); 423 K (brown) and 448 K (red).

As anticipated, a higher NaLe conversion is obtained as the temperature increases, reaching

69.2 % after 24 h at 448 K. As to the products, increasing total yields are obtained from 373 to

423 K, regardless of the reaction time (from 10.9 % to 37.3 % in the case of β-C10, and from 0.5

% to 13.2 % for δ-C10). However, this trend is broken at the highest temperature tested (448 K).

At this temperature, a maximum of 45.5 % total yield is obtained after 7 h, whereas this

magnitude decreases up to 16.6 % when reaction time is extended to 24 h. There is an

increasing discrepancy between FFL conversion and the total yield obtained. Thus, almost total

disappearance of FFL is observed at 448 K (99.6 % conversion after 24 h), whereas more than

80 % of this conversion is not explained by the product yields. In the same way, 17.8, 36.7 and

40.1 % of FFL conversions at 373, 393 and 423 K are not transformed into the target

compounds. These results discard the permanent adsorption without reaction (endothermic

character of adsorption but positive role of temperature in oligomerization reactions),

suggesting side reactions involving FFL leading to condensation. A high relevance of NaLe

oligomerization is almost disregarded, since the difference between NaLe conversion and total

yield is less than 6 % except at the highest temperature.

In order to corroborate the presence of different side reactions as function of the temperature,

the spent catalysts were analyzed by TPD, monitoring the evolution of individual signals of FFL,

LA, δ-C10 and β-C10 units (details in the *Experimental Section*). These results were compared

with individual saturation of fresh catalysts with NaLe and FFL. All the TPD traces are plotted in

the Supplementary Information (Figure S2), whereas the evolution of each adsorption is

analyzed in **Table 1** considering the values obtained at 373 K as baseline. Traces obtained at

temperatures below 450 K mainly correspond to reactants signals, with a relative weight of

products adsorption lower than 5 %. For FFL, the increase of the signal intensity observed as temperature increases corroborates the chemisorption, involving not only the adsorption but also oligomerization (promoted by the temperature). For the LA signal (direct correspondence with the NaLe one), a decrease in the adsorption is observed at low temperatures (congruent with physical adsorption), whereas there is an increase at the highest ones, suggesting oligomerizations. Results at 448 K clearly indicate a higher relevance of product signals; with the relative weight of δ-C10 being more than 6 times higher than those obtained at milder reaction conditions. These results support the initial hypothesis of side reactions involving products at temperatures of 448 K, Therefore, this temperature is discarded for future studies.

Table 1. TPD signal ratios as function of the reaction temperature taking the values of the lowest temperature as the baseline

T (K)	FFL (%)	LA (%)	β-C10 (%)	δ-C10 (%)
373	1.0	1.0	1.0	1.0
398	2.7	0.6	1.2	1.9
423	3.0	1.7	3.4	4.7
448	3.5	2.6	3.8	6.0

The influence of reaction temperature is also relevant in terms of reaction selectivity (Figure 2c), which shows the ratio β/δ decreases from 21.5 at 373 K to 2.1 at 448 K as the temperature increases. In the TPD analyses, δ-C10 signals are always higher than β-C10 ones (Fig. S2), i.e., in the opposite order than in liquid phase, suggesting that this isomer is preferentially adsorbed on the ZSM-5 surface.

All these data were used to propose, for the first time in the literature, a kinetic model for NaLe-FFL aldol condensation. According to the temporal evolution of all the compounds involved, and in good agreement with the previous literature, a first order kinetic is proposed for the compound that suffers the enolization (NaLe).[13,28,34,47] Previous studies of base catalyzed aldol condensations suggest that FFL is completely adsorbed on the surface, without any real influence on the kinetics (pseudo-zero order).[13,28] This assumption cannot be made in this case, since interactions between FFL and zeolites can be different, which also introduces its reaction order as a variable. The kinetic model is laid out in Scheme 1. To sum up, two parallel reactions are considered, k_1 and k_2 being the kinetic constants for the formation of β- and δ- adducts, respectively. Four other constants (k_{D_LA} for NaLe, k_{D_FFL} for FFL, $k_{D\_β}$, and $k_{D\_δ}$ for C10s) represent the effects of the adsorption and oligomerization of reactants and products on the catalyst surface. The kinetic orders for these lateral processes are also included in the model. A differential equations system is proposed, assuming an ideal batch reactor.

$$\frac{d(NaLe_{1:1})}{dt} = -k_1 \cdot C_{NaLe_{1:1}} \cdot C_{FFL_{1:1}}^m - k_2 \cdot C_{NaLe_{1:1}} \cdot C_{FFL_{1:1}}^m - k_{D_{NaLe}} \cdot C_{NaLe_{1:1}}^n \quad (4)$$

$$\frac{d(FFL_{1:1})}{dt} = -k_1 \cdot C_{NaLe_{1:1}} \cdot C_{FFL_{1:1}}^m - k_2 \cdot C_{NaLe_{1:1}} \cdot C_{FFL_{1:1}}^m - k_{D_{FFL}} \cdot C_{FFL_{1:1}}^p \quad (5)$$

$$\frac{d(\beta - C10_{1:1})}{dt} = k_1 \cdot C_{NaLe_{1:1}} \cdot C_{FFL_{1:1}}^m - k_{D_\beta} \cdot C_{\beta-C10_{1:1}}^q \quad (6)$$

$$\frac{d(\delta - C10_{1:1})}{dt} = k_2 \cdot C_{NaLe_{1:1}} \cdot C_{FFL_{1:1}}^m - k_{D_\delta} \cdot C_{\delta-C10_{1:1}}^r \quad (7)$$

As some of variables are related to kinetic orders, experiments with different initial reactant ratios had to be carried out. Assuming that most of the side reactions involve FFL, different excesses of NaLe were studied (2:1, 5:1), being the main results compared to those obtained

with 1:1 in **Figure 3**. For these studies, temperature was fixed at 423 K, this value being the optimum one obtained in the previous screening. The increase in final FFL conversion and the decrease in NaLe conversion were as expected, according to their conditions of limiting and excess reactant, respectively. The most relevant aspect is the evolution of the carbon balance, with a constant increase as NaLe excess increases (76.8, 91 and 97.1 %, at 1:1, 2:1, and 5:1, respectively). Thus, more than 40 % of FFL converted at 1:1 is not transformed into products. This percentage is reduced to 25 and 0 % when working at 2:1 and 5:1, respectively. However, at 5:1, 8 % of NaLe converted is not observed in the reaction products, suggesting that a high excess of NaLe is also detrimental, as this promotes side reactions involving this acid. As to the products, the branched product is the main one under all the conditions tested, reaching the maximum selectivity at 2:1. At these conditions, the ratio β/δ increases from 2.8 (1:1) to 5.8 (2:1), decreasing to 3.4 when working at 5:1. In overall terms, working at 5:1 also implies a decrease in the total yield, reaching a maximum of 42.5 %, whereas 50 % is obtained at 1:1 and 2:1.
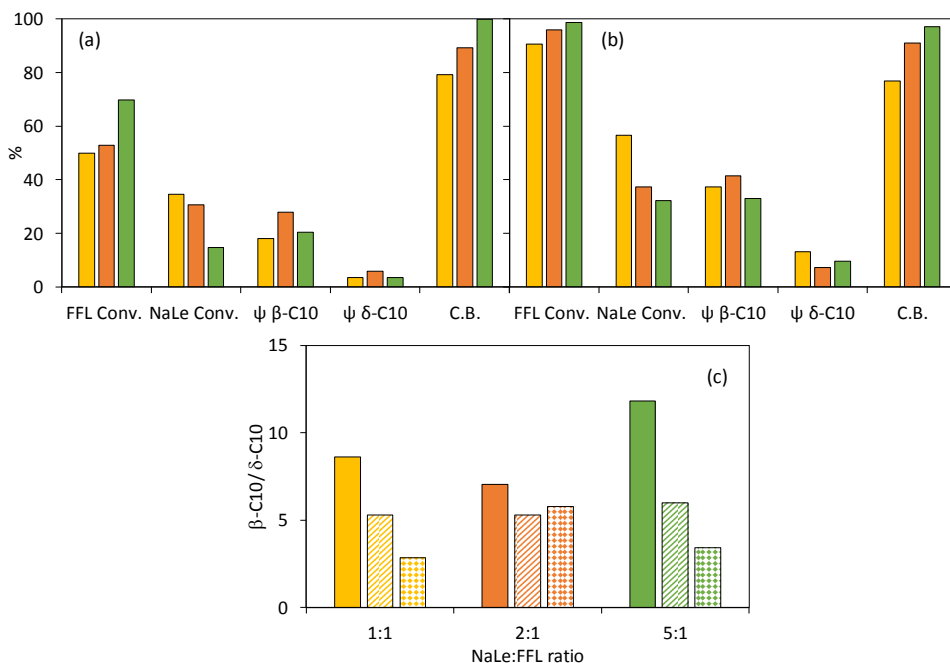
Figure 3. Summary of results obtained for the NaLe-FFL aldol condensation catalysed by 1.8 g of ZSM-5 (23) as a function of the reactants ratio and the reaction time (423 K). Legend: (a) 8 h, (b) 24h and (c) products ratio at different times: 4 h (solid columns), 8 h (dashed columns) and 24 h (diamond columns); 373 K (blue); 1:1 (yellow); 2:1 (orange) and 5:1 (green).

These results were considered -together with the temperature influence- implemented in the kinetic model. The proposed model was solved numerically using MATLAB code, performing all the calculations and solving the set of ordinary differential equations ("ode45"). The fitting of the unknown parameters from the model is accomplished by the least-square method. The MATLAB function "lsqcurvefit" using the Levenberg-Marquardt algorithm was used. The coefficient of determination was calculated with MATLAB function "rsquare". **Figure 4** shows the good fit of the proposed model, whereas **Table 2** summarizes the values of the kinetic and adsorption constants for all the conditions studied, as well as the activation energy obtained by applying the Arrhenius equation.
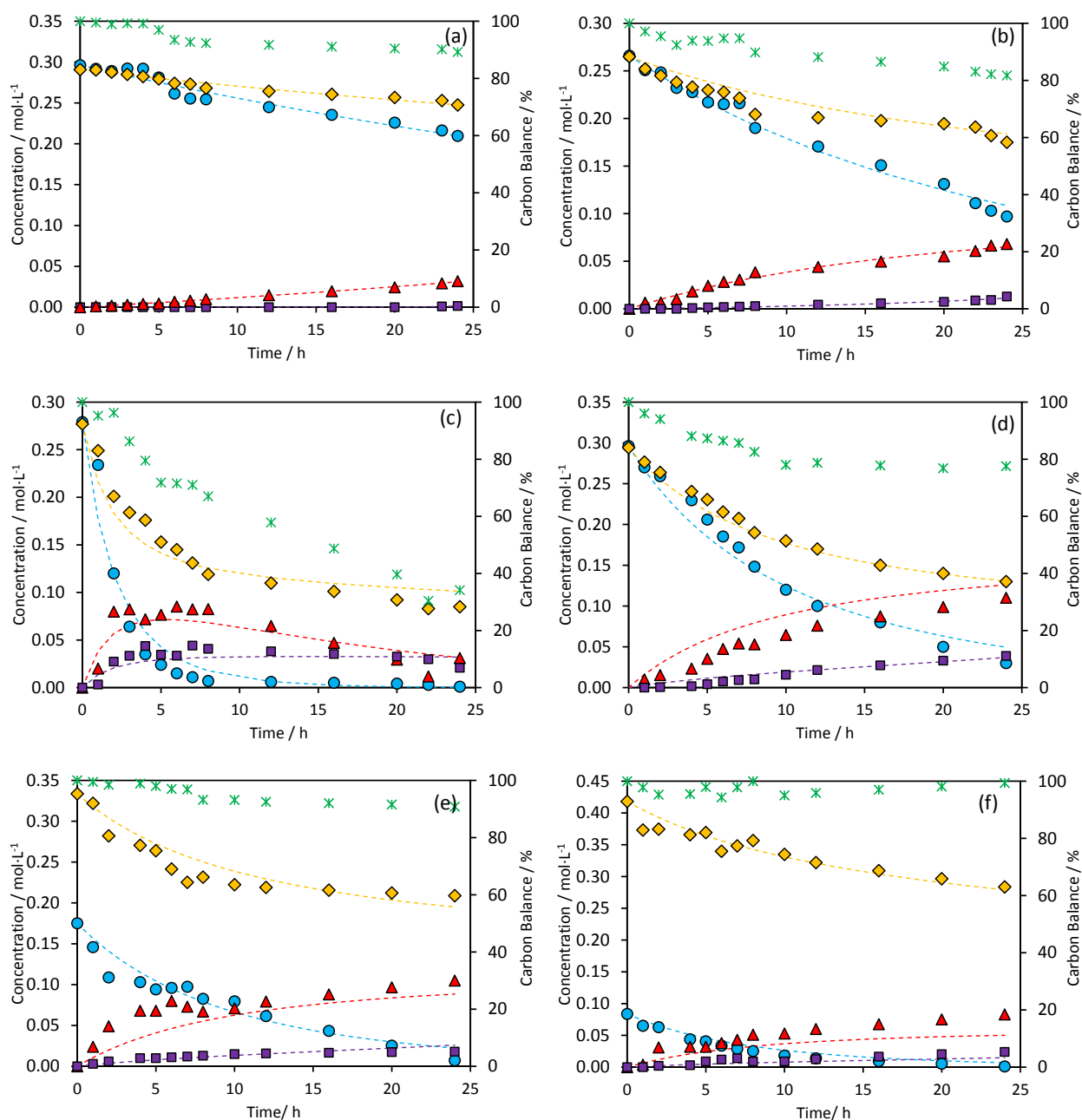
Figure 4. Kinetic fitting for different conditions studied in terms of temperature and NaLe:FFL ratio. Results correspond to: (a) 398 K, 1:1; (b) 403 K, 1:1; (c) 448 K, 1:1; (d) 423 K, 1:1; (e) 423 K, 2:1; (f) 423 K, 5:1. Legend: (a) 398 K; (b) 423 K, and (c) 448 K. Experimental points plotted with different symbols, whereas broken lines corresponds to kinetic model predictions. Symbols: (♦) NaLe; (●) FFL; (▲) β-C10; (■) δ-C10 and (∗) carbon balance.

Table 2. Rate and adsorption constants for the fitting of the experimental results to the proposed kinetic model at different temperatures and 1.8 g of ZSM- 5 (23). K_{D_β} and k_{D_δ} are only reported at the highest temperature, in other cases, this value is less than 0.001. The activation energy for k_{D_LA}, k_{D_FFL}, k_{D_β} and k_{D_δ} has not been calculated as these constants are not intrinsic kinetic parameters of the target reaction.

	k_1 (L·h⁻¹·mol⁻¹)	k_2 (L·h⁻¹·mol⁻¹)	k_{D_NaLe} (L$^{1.5}$·h⁻¹·mol⁻¹·⁵)k2	k_{D_FFL} (h⁻¹)k3	k_{D_β} (h⁻¹)	k_{D_δ} (h⁻¹)	r^2
373 K	0.013	0.000	0.026	0.013	-	-	0.999
398 K	0.076	0.003	0.038	0.026	-	-	0.992
423 K	0.198	0.036	0.056	0.043	-	-	0.985
448 K	0.725	0.249	0.273	0.271	0.054	0.003	0.958
Ea (kJ·mol⁻¹) r^2	72.7 0.992	128.0 0.999	-	-	-	-	-

In general terms, proposed model adequately fits the experiments performed at different reactant ratios and temperatures, obtaining a total determination coefficient of 0.982. A first kinetic order of FFL was obtained for both direct reactions (experimental value of 0.94). This result indicates a weaker interaction between FFL and the zeolitic surface than when working with basic catalysts (zero-th order[13,28]). In good agreement with this hypothesis, side reactions involving this product disappear when increasing the NaLe:FFL ratio, whereas they were always relevant when working with basic conditions.[13,28] In the same way, a first order kinetic for FFL was obtained for the lateral reactions involving FFL and both products, suggesting side processes concerning permanent adsorption with a limited oligomerization. Lateral reactions of both products are only relevant at the highest temperature tested (448 K). On the contrary, the side reaction of NaLe has a 2.5 order and a relevant kinetic constant. The high kinetic order obtained as well as the almost absence of real effects of this undesired reaction, except in the

case of the highest levulinic excess (5:1), suggests that side reaction involving NaLe is a complex step not only determined by the concentration of NaLe but also by some intermediates not quantified in the liquid phase. This hypothesis requires more experiments to be corroborated (see *Catalyst performance* section).

The rate constants obtained follow a perfect Arrhenius dependence with the temperature, obtaining an activation energy for the branched product (C10) almost fifty percent lower than the one obtained for the linear adduct. This result explains the increasing differences observed in both profiles as the temperature decreases, with an almost total disappearance of C10 at temperatures lower than 393 K.

Catalyst performance of different zeolites

Two main parameters are analysed in this section: the influence of acidity, by comparing the activity of two different ZSM-5 zeolites with different SiO_2/Al_2O_3 ratio; and the influence of catalyst's structure, by comparing the activity of the ZSM-5 zeolite with BETA and Mordenite. In both cases, the study is focused on the activity, but also selectivity to the main reaction products. All reactions are carried out at 398 K with a NaLe:FFL initial ratio of 1:1.

<u>Influence of surface acidity</u>

The role of surface acidity was studied comparing the activity of two ZSM-5 zeolites with different SiO_2/Al_2O_3 ratio: 23 and 80. Experimental results are analysed in **Figure 5.**
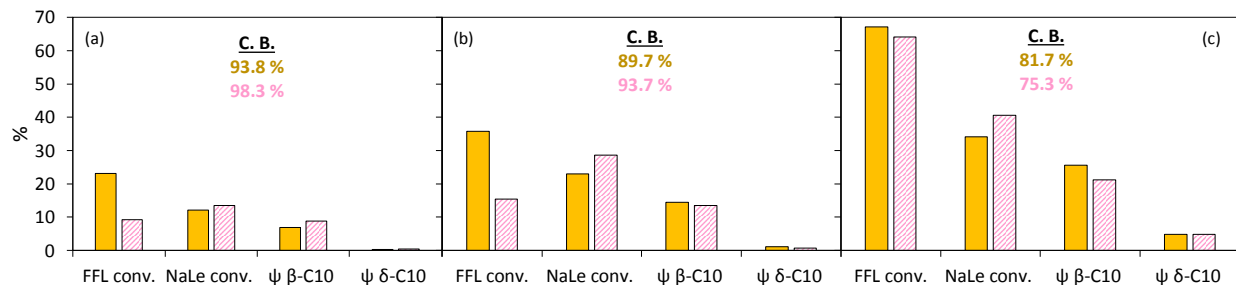
Figure 5. Summary of results obtained from the NaLe-FFL aldol condensation using equimolar reactants ratio at 398 K and catalysed by 1.8 g of ZSM-5 with different SiO_2/Al_2O_3 ratio: 23 (solid columns) and 80 (dashed columns). Symbols: (a) 4 h; (b) 8 h and (c) 24 h.

The main differences are related to the disappearance of FFL at low reaction times (4 h) being more than three times higher in the case of the ZSM-5 (23). This fact is congruent with the existence of a higher concentration of acid sites, as it is reported in **Table 3**, and its promotion of adsorption processes. As anticipated, the different acidity is the main morphological difference between both materials, since both zeolites have the same framework structure (intersecting straight and sinusoidal channels by 10-membered oxygen ring). However, the different Si/Al distribution on the surface also affect to the external surface, being 25 % higher in the case of the less acidic material.

24

Table 3. Textural and acidic properties of zeolite materials. BET, surface area from BET method; V_{micro}, microporevolume from t-plot method; V_{meso}, mesopore volume (from BJH method); $D_{Howartz}$, average pore diameter for microporous materials.

Catalyst	BET $(m^2 \cdot g^{-1})$	S_{ext} $(m^2 \cdot g^{-1})$	V_{micro} $(cm^3 \cdot g^{-1})$	V_{meso} $(cm^3 \cdot g^{-1})$	$D_{Howartz}$ (Å)	Total acidity $(\mu mol\ NH_3 \cdot g^{-1})$	% of weak acidity $(T_{des} < 560\ K)$	Total acidity $(meqH^+ \cdot g^{-1})$
ZSM-5 (23)	353	109	0.12	0.07	8.0	350.3	65.5	2.49
ZSM-5 (80)	440	199	0.12	0.06	8.2	17.31	85.4	0.26
MOR (20)	440	59	0.18	0.08	8.8	139.5	65.5	1.35
BETA (25)	620	243	0.18	0.73	10.2	210.0	72.6	1.69

The reaction is more selective for the condensation products at short times with the ZSM-5 (80) with better correspondence between FFL and products evolutions. β-C10 is the main compound obtained with both materials (7.2 and 9.2 %), whereas the yield of δ-C10 is almost negligible after only 4 h (0.3 and 0.4 %, for ZSM-5 (23) and ZSM-5 (80), respectively). All these experimental results are in good agreement with the rate constants obtained by the same method as before and are listed in **Table 4**. Opposite behaviors are observed at increasing times. Thus, the total products yield after 8 h is slightly higher for the most acidic zeolite (15.6 % *vs.* 14.2 %), reaching a 17 % higher yield after 24 h (30.5 % *vs.* 26 %). The selectivity between both adducts is also different, with the final mixture obtained with the ZSM-5 (80) being enriched in the linear one (β/δ final ratios of 5.2 and 4.4, respectively). Similar evolutions of FFL conversion are obtained in both cases, with final conversions of 67 and 64 %. On the contrary, significant differences are observed with the levulinate: whereas there is almost a complete correspondence between its conversion and the product yields with ZSM-5 (23), there is more than 15 % of discrepancy in the case of the ZSM-5 (80). All these experimental results are in good agreement with kinetic values obtained. Thus, the production of linear

adduct is enhanced when decreasing the acidity (k_2 is 2.7 times higher), whereas the branched

one, identified with the k_1, slightly decreases (10 %). Moreover, FFL side reactions are

promoted by the acidity, but this increase is negligible in comparison with the promotion of

side reactions involving NaLe in the case of the ZSM-5 (80), as it is observed with a k_{D_NaLe} 7.4

times higher than with the ZSM-5 (23).

Carbon balance closures obtained follow the expected evolution according to data previously

discussed. At short reaction times (4 h), almost 100 % is obtained with the ZSM-5 (80), whereas

with the ZSM-5 (23) this parameter is close to 90 % (93.8%). On the contrary, opposite

behaviors are observed at long reaction times. A continuous and gradual decrease to 82 % is

observed with the most acidic material. However, the carbon balance decreases to 75 % with

the ZSM-5 (80), this decrease being promoted only at long reaction times (it keeps almost

constant over 94 % during the first 8 h). This behavior is congruent with the previous hypothesis

that deactivation due to NaLe is not directly related to this compound but to a non-identified

product involving this molecule (or other derivative obtained by a non-catalytic process) and

the linear product (δ-C10). This assumption is based on two pieces of evidence: on the one

hand, the small difference between δ-C10 with both materials does not correspond with the

relevance difference in the rate constants, which is congruent with the existence of other steps

involving δ-C10 as reactant. On the other hand, TPO analyses of spent catalyst suggests the

presence of a totally different type of solids deposed on the catalytic surface of the ZSM-5 (80),

as it is observed in **Fig. S3**. Traces obtained during the oxidation of ZSM-5 (23) have two main

peaks, at 587 and 625 K. The first one is also observed with the ZSM-5 (80), being assigned to

FFL oligomers (common side reaction observed in both cases with higher relevance with the

zeolite). However, the second peak does not appear in the TPO of ZSM-5 (80), being substituted by a main peak at 710 K. This peak demonstrates the existence of a different reaction, not observed with the ZSM-5 (23).

This undesired reaction observed with the less acidic material suggests that the key parameter is not the total amount, but also the acid strength distribution of these sites. NH_3-TPD analyses of fresh materials (**Fig. S4**) indicate the existence of two types of acid sites: weak and medium strength ones (desorption temperatures from 298 to 560 K for the weak acids, and from 560 to 820 K for medium sites). ZSM-5 (23) has a total concentration of acid sites 20 times higher than the one of ZSM-5 (80). In addition, 34.5 % of these sites are medium strength sites, whereas this percentage decreases to less than 14 % in the case of ZSM-5 (80). It is well known that internal carbons are nucleophilic centers stronger than the terminal ones. According to this, the protons of these internal carbons are easily abstracted since they are more acidic than the terminal ones (always comparing only C-H bonds). These protons play a key role once the carbonyl is protonated, since one of them must be abstracted from the levulinate to generate the enol and restore the electro-neutrality of the zeolitic material (tautomerization step). The proton abstraction must be catalyzed by a basic acid site (the free oxygen of the silanol group produced once the H has passed to the NaLe structure). The more electropositive hydrogen, the weaker basicity required to remove it, and the stronger conjugated acidity associated to it. According to this, the catalyst that enhances the production of the linear compound must have a higher percentage of weak acidity, since the conjugated stronger basic site is required to stabilize the intermediate obtained. On the contrary, removing the α-hydrogen of the C3 position only requires medium-weak basicity, corresponding to medium acidity of the silanol

group. In good agreement with this analysis, the β/δ ratio is higher with the zeolite enriched in medium-strength acidic sites, ZSM-5 (23), mainly at short times (286 *vs.* 51.7).

Structure influence

Figure 6 shows the results obtained for the FFL-NaLe aldol condensation reaction after (a) 8 h, and (b) 24 h of performing the aldol condensation at 398 K with three different zeolites: ZSM-5 (23); mordenite, labelled as MOR (20); and beta zeolite, identified as BETA (25).
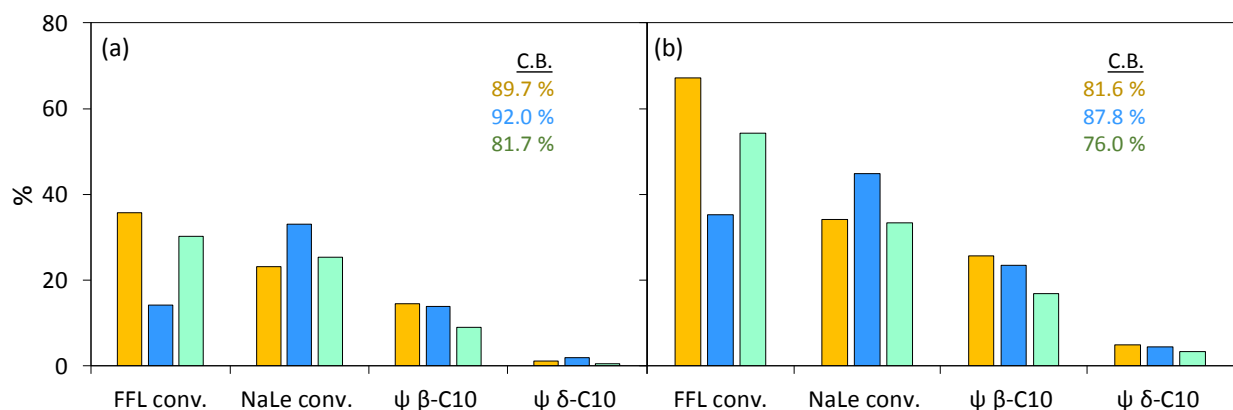
Figure 6. Summary of results obtained of NaLe-FFL aldol condensation at 398 K and catalysed by 1.8 g of different zeolites as function of the reaction time (equimolar reactants ratio): (a) 8 h and (b) 24h . Legend: ZSM-5 (23) (yellow); MOR (blue) and BETA (green).

In this case, conclusions drawn after 8 h can be directly applied to the analysis at 24 h (opposite situation than what happened with the acidity comparison). The lowest FFL conversion (35.2%) is obtained with MOR, while the values for BETA and ZSM-5 are 54.2, 63.5 %, respectively. As to NaLe, the highest conversion is reached with MOR (44.8 %), whereas similar values where quantified for BETA and ZSM-5 (34.1 and 33.4 %, respectively). The maximum C10 total yield is obtained with ZSM-5 (30.5 %), very similar yield than the corresponding value with MOR (27.9 %). On the contrary, the total yield obtained with BETA is significantly lower (20.3 %) than

the one obtained with ZSM-5. This value is 33 % lower than the obtained with ZSM-5, despite

giving similar conversions of both reactants. In all the cases, the branched adduct (β-C10) is

obtained in higher amounts than the linear one (δ-C10), these differences being more

pronounced at short reaction times. Thus, initial β/δ ratios of 286, 249 and 21 for ZSM-5, MOR

and BETA during the first two hours decrease to 5.2, 5.1 and 5.4 after 24 h, respectively. These

results are in good agreement with the percentage of weak acid sites (strong conjugated bases)

of these materials, as observed in Table 3. According to these results, the best selectivity for

desired compounds seems to be observed with the MOR, with side reactions taking place to a

lower extent. Considering the calculated kinetic constants (see **Table 4**), this material almost

prevents FFL side reactions (k_{D_FFL} 13 times lower than the ones obtained with ZSM-5 and

BETA). This value is in good agreement with the low FFL disappearance not explained by the

C10 formation (more than 5 times lower than values with the other materials).

Table 4. Rate and adsorption constants for the fitting of the experimental results to the proposed kinetic model using different zeolites at 398 K and the values for MOR at different temperatures. K_{D_β} and k_{D_δ} are only reported at the highest temperature, in other cases, this value is less than 0.001. Activation energy for k_{D_NaLe}, k_{D_FFL} and k_{D_β} and k_{D_δ} has not been calculated as these constants are not intrinsic kinetic parameters.

Catalyst	T (K)	k_1 (L·h⁻¹·mol⁻¹)	k_2 (L·h⁻¹·mol⁻¹)	k_{D_NaLe} (L^{1.5}·h⁻¹·mol⁻¹·⁵)k2	k_{D_FFL} (h⁻¹)k3	k_{D_β} (h⁻¹)	k_{D_δ} (h⁻¹)	r^2
ZSM-5 (23)		0.076	0.003	0.038	0.026	-	-	0.992
ZSM-5 (80)	398	0.067	0.008	0.125	0.022	-	-	0.992
BEA (25)		0.053	0.006	0.107	0.027	-	-	0.995
	398	0.064	0.009	0.184	0.003	-	-	0.991
MOR (20)	423	0.285	0.068	0.202	0.011	-	-	0.970
	448	0.637	0.101	0.257	0.019	0.049	0.013	0.941
Ea (KJ·mol⁻¹)		68.3	72.1	-	-	-	-	-
r^2		0.981	0.892					

These kinetic constant values are obtained applying the same mechanism proposed for the ZSM-5, supporting the hypothesis of same reaction pathway despite the catalytic structure used. The goodness of this fit is shown in **Figure 7**.
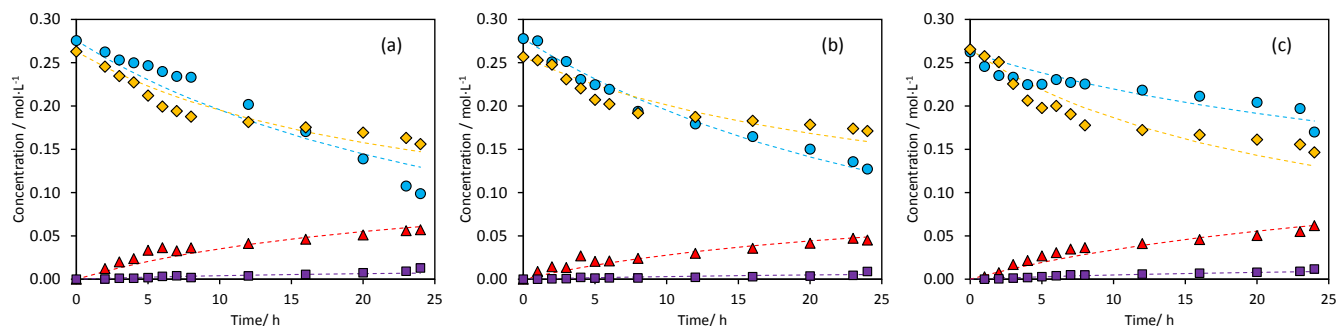

Figure 7. Kinetic model predictions for NaLe:FFL (1:1) condensation at 423 K as function of the catalyst. Results correspond to: (a) ZSM-5 (80); (b) BETA; (c) MOR. Experimental points plotted with different symbols, whereas broken lines corresponds to kinetic model predictions. Symbols: (♦) NaLe; (●) FFL; (▲) β-C10; (■) δ-C10.

BETA zeolite was discarded because of the low final yields, but the goodness of the fit for MOR is not so clear, due to the high k_{D_NaLe} obtained (almost 11 times higher than with the ZSM-5). In good agreement with this value, the amount of NaLe not converted into C10s is almost 5 times higher than the one with ZSM-5.

In order to check if the negative consequences of these side reactions, previously suggested in the acidity study, prevail over the positive effect of almost preventing FFL oligomerization, reactions at different temperatures with MOR have been carried out. The main results after 24 h are compared in **Figure 8**, whereas the temporal evolution, as well as the kinetic prediction is included in the Supplementary Information (Figure S5). Results at 448 K are discarded according to the low carbon balance closure (33.6 %). However, values obtained at 423 K are

significantly worse than those obtained with ZSM-5 (23), obtaining a carbon balance of 61 %

(compared to 77.5 % with the ZSM-5). This carbon balance is explained by the lateral reactions

involved NaLe (high increase in the disappearance of this reactant despite the decrease in the

C10 yields) and the higher selectivity to δ-C10 adduct (β/δ ratio of 14, whereas a value of 25

was obtained with the ZSM-5). In summary, ZSM-5 is considered to be the best material since

its higher activation energy for the linear adduct production (128 *vs.* 72.1 kJ·mol^{-1}) prevents a

fast production of the linear isomer and the side reactions involving it (as expressed by k_{D-NaLe}).
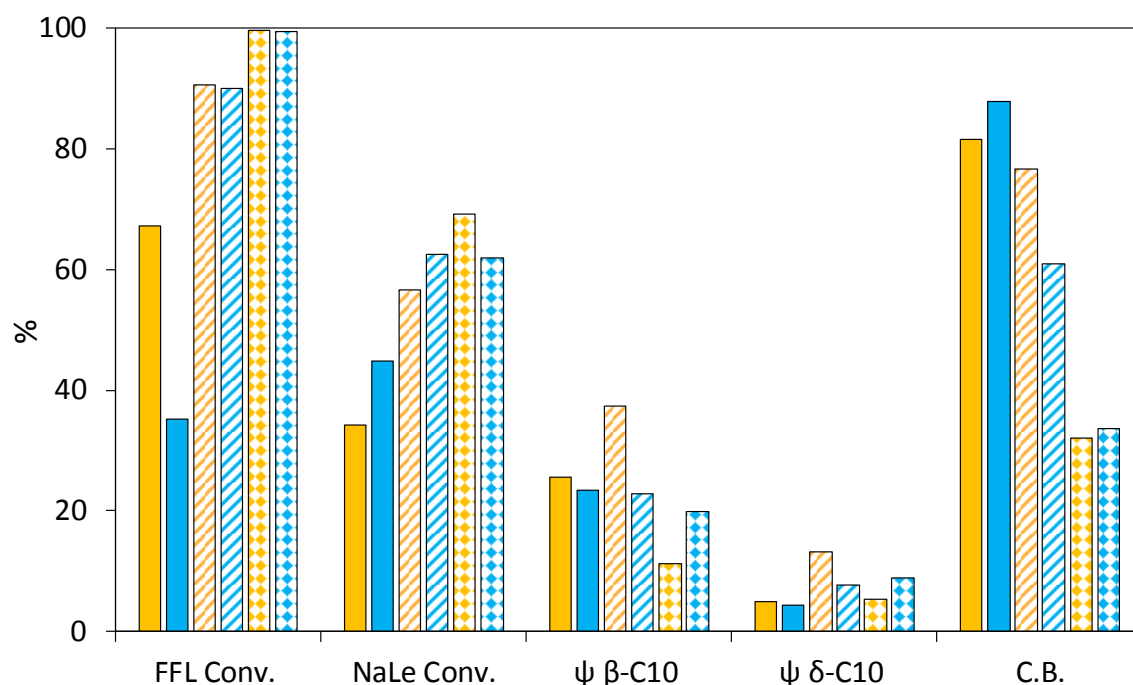
Figure 8. Comparison of results obtained of NaLe-FFL aldol condensation at 398 K and catalysed
by 1.8 g of different zeolites as function of the reaction time (equimolar reactants ratio, 24 h).
Legend: ZSM-5 (23) (yellow) and MOR (20) (blue); 398 K (solid bars), 423 K (dashed bars) and
448 K (diamond bars)

The different behaviours of these three zeolites cannot be explained as function of their

morphological properties since there is not any clear correlation between external surface,

total one, or pore volume with the activity results (Table 3). Therefore, it can be concluded that this reaction is not sensitive to the zeolite structure. Instead, the distribution of the acid sites is the key parameter. Thus, an increase in the percentage of weak acid sites has a negative effect on the overall outcomes. There is a linear correlation between k_1 and k_2 and this type of acid sites with opposite trends (they promote the production of linear adduct, preventing the branched one). In good agreement, a clear decrease in the β/δ ratio with this acidity is obtained. On the contrary, the lateral reactions involving NaLe increase with the percentage of weak acid sites, whereas there is not any clear trend concerning the lateral reactions involving FFL. **Figure 9** illustrate these evolutions.

As a summary of the previous analysis, the best conditions require working with ZSM-5 (23) at 423 K. While side reactions involving NaLe are minimized, these conditions also favoured FFL oligomerization because of the high amount of medium-strength acid sites. Consequently, a low excess of LA is required to obtain the optimum activity (2:1) as it was previously demonstrated.

Catalyst stability

Stability tests were carried out employing the optimum conditions previously determined (24 h, 423 K, 2:1 NaLe:FFL reactant ratio and ZSM-5 (23) catalyst). After each cycle the catalyst was recovered by filtration, washed with water and dried overnight at 373 K, without applying any further regeneration procedure between cycles. **Figure 10** shows the main results after four cycles.
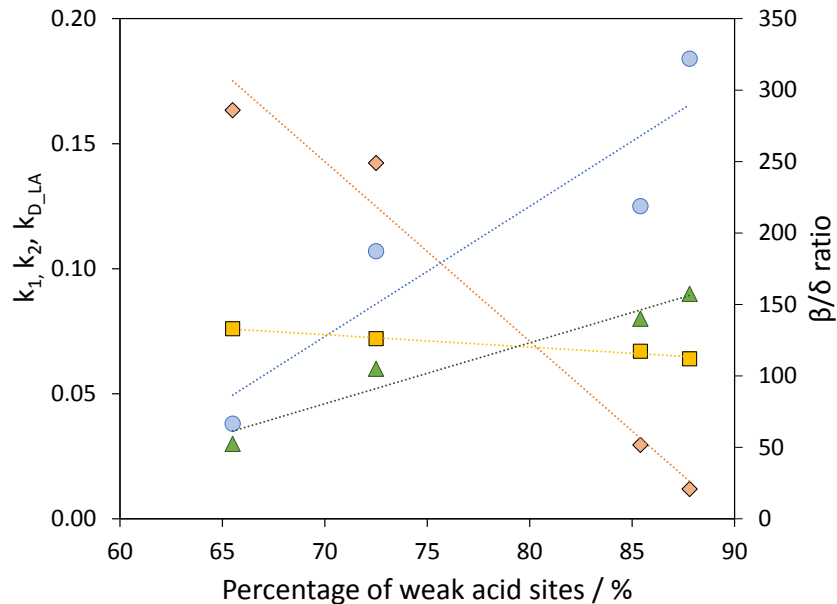
Figure 9. Evolution of different parameters with the relative percentage of weak acid sites presents in each material. Symbols: (■) k_1; (▲) k_2 (x10); (●) k_{D_NaLe}; (♦) β/δ ratio at initial times.

A decrease of less than 10 % in FFL conversion is observed (95 *vs.* 89 %, after the first and fourth cycle, respectively). Almost 60 % of the total C10 obtained in the first cycle are still produced in the fourth one, with the β-C10 adduct suffering a larger decrease in its productivity. A gradual, but continuous decrease in the carbon balance closure (87.5 % after the fourth cycle) as well as the increasing discrepancy between reactant conversions and products yields is congruent with the deposition of these adducts as the main deactivation cause. At this point, it should be noted that the deactivation is markedly lower than in other reported condensation reaction, and that the deactivated catalyst can be fully regenerated by air treatment. TPO results also show that carbonaceous can be burned off below 800 K, with the structure of the ZSM-5 being stable at this temperature.
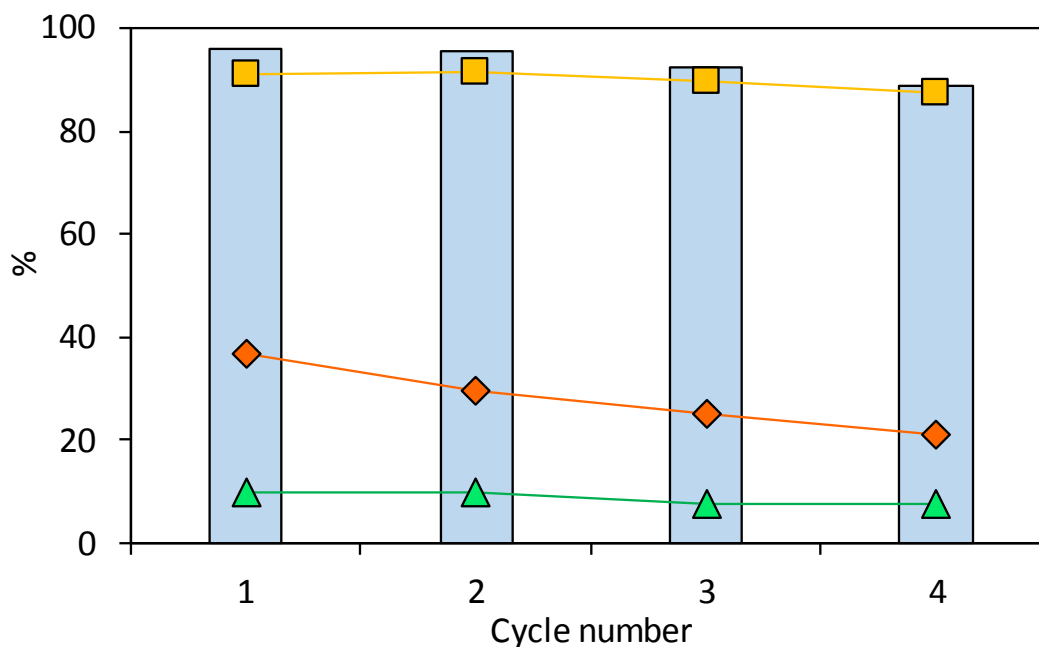
Figure 10. Reusability results after 24 h of each cycle at 423 K, using ZSM-5 (23) and 2:1 as NaLe:FFL ratio. Legend: (blue bars) FFL conversion; (■) Carbon Balance; (♦) β-C10 yield; (▲) δ- C10 yield.

CONCLUSIONS

Promising results are obtained in the furfural and levulinic acid aldol condensation catalysed with acid zeolites. A prior neutralization of the carboxylic group of LA is required to prevent the cyclization, obtaining good activity results when using Na_2CO_3, obtaining the sodium levulinate. A deep study of reaction conditions was carried out, concluding that optimum values correspond to 423 K, and an initial NaLe:FFL ratio 2:1. ZSM-5 (23) is identified as the best catalyst tested, realizing more than 50 % of total yield (two C10 products obtained) with a good carbon balance closure (92 %). A kinetic model is proposed, suggesting furfural oligomerization

as the main deactivation cause, as well as a negative interaction between NaLe excess and a high production of the linear adduct (δ-C10). The acidity strength is identified as the key parameter to prevent this side reaction, being directly related to the prevalence of weak acid sites.

ASSOCIATED CONTENT

Supporting Information

The Supporting Information is available at

It includes: Fig. S1: m/z spectra of each compound involved in the reaction; Fig. S2: TPD analyses of spent catalyst; Fig. S3: TPO analyses of spent catalysts; Fig. S4: NH_3-TPD of different zeolites; and Fig. S5: the temporal evolution and kinetic prediction of results obtained with MOR at different temperatures.

AUTHOR INFORMATION

Corresponding Author

*e-mail: sordonez@uniovi.es, Tel: +34 985 103 437; Fax: + 34 985 103 434

Author Contributions

The manuscript was written through contributions of all authors. All authors have given

approval to the final version of the manuscript.

REFERENCES

(1)   Hilali, S.; Fabiano-Tixier, A.S.; Ruiz, Z.; Hejiaj, Al.; Nouh, F.A.; Idlimam, A.; Bily, A.; Mandi,

L.; Chemat, F., Green extraction of essential oils, polyphenols and pectins from orange

peel employing solar energy: toward a zero-waste biorefinery. *ACS Sust. Chem. Eng*. **2019**,

7, 11815-11822. Doi: 10.1021/acssuschemeng.9b02281.

(2)   Han, X.; Guo, Y.; Liu, X.; Xia, Q.; Wang, Y., Catalytic conversion of lignocellulosic biomass

into hydrocarbons: A mini review. *Catal. Today* **2019**, 319, 2-13. Doi:

10.1016/j.cattod.2018.05.013.

(3)   Malkar, R.S.; Daly, H.; Hardacre, C.; Yadav, G.D., Aldol condensation of 5-

hydroxymethylfurfural to fuel precursors over novel aluminum exchanged-DTP@ZIF-8.

ACS Sust. Chem. Eng. **2019**, 7, 16215-16224. Doi: 10.1021/acssuschemeng.9b02939.

(4)   Yutthalekha, T.; Suttipat, D.; Salakhum, S.; Thivasasith, A.; Nokbin, S.; Limtrakul, J.;

        Wattankit, C., Aldol condensation of biomass-derived platform molecules over amine-

        grafted hierarchical FAU-type zeolite nanosheets (Zeolean) featuring basic sites. *Chem.*

        Commun. **2017**, 53, 12185-12188. Doi: 10.1039/c7cc06375j.

(5)   Barrett, C.J.; Chheda, J.N.; Huber, G.W.; Dumesic, J.A., Single-reactor process for

        sequential aldol-condensation and hydrogenation of biomass-derived compounds in

        water. *Appl. Catal. B* **2006**, 66, 111-118. Doi: 10.1016/j.apcatb.2006.03.001.

(6)   Chheda, J.N.; Dumesic, J.A., An overview of dehydration, aldol-condensation and

        hydrogenation processes for production of liquid alkanes from biomass-derived

        carbohydrates. *Catal. Today* **2007**, 123, 59-70. Doi: 10.1016/j.cattod.2006.12.006.

(7)   Dowson, G:R.M.; Haddow, M.F.; Lee, J.; Wingad, R.L.; Wass, D.F., Catalytic conversion of

        ethanol into an advanced biofuel: unprecedented selectivity for n-butanol. Angew. Chem.

        Int. Ed. 2013, 52, 9005-9008. Doi: 10.1002/anie.201303723.

(8)   Silks, L.A.; Gordon, J.C.; Wu, R.; Hanson, S.K., Process for preparation of furan derivatives

        by carbon chain extension through aldol reaction. WO2011022042A1, 2011.

(9)   Yadav, G.D.; Yadav, A.R., Novelty of Claisen-Schmidt condensation of biomass derived

        furfural with acetophenone over solid super base catalyst. *RSC Adv*. **2014**, 4, 63772-

        63778. Doi: 10.1039/c4ra09194a.

(10)   Rapeyko, A.; Arias, K.S.; Climent, M.J.; Corma, A.; Iborra, S., Polymers from biomass: one pot two-step synthesis of furilydenepropanenitrile derivatives with MIL-100(Fe) catalyst. *Catal. Sci. Technol.* **2017**, 7, 3008-3016. Doi: 10.1039/c7cy00463j.

(11)   Siewert, R.; Zaitsau, D.H.; Emel'yanenko, V.N.; Verevkin, S.P., Biomass valorization: thermodynamics of the Guerbet condensation reaction. *J. Chem. Eng. Data* **2019** *(in press)*. Doi: 10.1021/acs.jced.9b00419.

(12)   Gordon, J.C.; Silks, L.A.; Sutton, A.D.; Wu, R., Schalf, M.; Waldie, F.; West, R.; Collias, D.I., Compounds and methods for the production of long chain hydrocarbons from biological sources. WO2013040311A1, 2013.

(13)   Cueto, J.; Faba, L.; Díaz, E.; Ordóñez, S., Performance of basic mixed oxides for aqueous-phase 5-hydroxymethylfurfural-acetone aldol condensation. *Appl. Catal. B* **2017**, 201, 221-231. Doi: 10.1016/j.apcatb.2016.08.013.

(14)   Xu, J.; Li, L.; Li, G.;Wang, A; Cong, Y.; Wang, X.; Li, N., Synthesis of renewable C8-C10 alkanes with angelica lactone and furfural from carbohydrates. *ACS Sust. Chem. Eng.* **2018**, 6, 6126-6134. Doi: 10.1021/acssuschemeng.7b04797.

(15)   Kikhtyanin, O.; Kubicka, D.; Cejka, J., Toward understanding of the role of Lewis acidity in aldol condensation of acetone and furfural using MOF and zeolite catalyst. *Catal. Today* **2015**, 243, 158-162. Doi: 10.1016/j.cattod.2014.08.016.

(16) Xiang, M.; Liu, J.; Fu, W.; Tang, T.; Wu, D., Improved activity for cellulose conversion to levulinic acid through hierarchization of ETS-10 zeolite. *ACS Sust. Chem. Eng.* **2017**, 5, 5800-5809. Doi: 10.1021/ acssuschemeng.7b00529.

(17) Yan, K.; Jarvis, C.; Gu, J.; Yan, Y., Production and catalytic transformation of levulinic acid: A platform for specialty chemicals and fuels. *Renew. Sust. Energ. Rev.* **2015**, 51, 986-997. Doi: 10.1016/j.rser.2015.07.021.

(18) Pileidis, F.D.; Titirici, M.M., Levulinic acid biorefineries: new challenges for efficient utilization of biomass. *ChemSusChem* **2016**, 9, 562-582. Doi: 10.1002/cssc.201501405.

(19) Mellmer, M.A.; Gallo, J.M.R.; Martín Alonso, D.; Dumesic, J.A., Selective production of levulinic acid from furfuryl alcohol in THF solvent systems over H-ZSM-5. *ACS Catal.,* **2015**, 5, 3354-3359. Doi: 10.1021/acscatal.5b00274.

(20) Orlowski, I.; Douthwaite, M.; Iqbal, S.; Hayward, J.S.; Davies, T.E.; Bartley, J.K.; Miedziak, P.J.; Hirayama, J., The hydrogenation of levulinic acid to γ-valerolactone over Cu-ZrO2 catalysts prepared by a pH-gradient methodology. *J. Energ. Chem*. **2019**, 36, 15-24. Doi: 10.1016/j.jechem.2019.01.015.

(21) Murugesan, K.; Aslhammari, A. S.; Sohail, M.; Jagadeesh, R. V., Levulinic acid derived reusable cobalt-nanoparticles-catalyzed sustainable synthesis of γ-valerolactone. *ACS Sust. Chem. Eng.* **2019**, 7, 14756-14764. Doi: 10.1021/acssuschemeng.9b02692.

(22) Lilga, M.A.; Padmaperuma, A.B.; Auberry, D.L.; Job, H.M.; Swita, M.S., Ketonization of levulinic acid and valerolactone to hydrocarbon fuel precursors. *Catal. Today* **2018**, 302, 80-86. Doi: 10.1016/j.cattod.2017.06.021.

(23) Horváth, I.; Mehdi, H.; Fábos, V.; Mika, L.T., Valerolactone – a sustainable liquid for energy and carbon-based chemicals. *Green Chem.* **2008**, 10, 238-242.

(24) Schuette, H.A.; Thomas, R.W., Normal valerolactone III. Its preparation by the catalytic reduction of levulinic acid with hydrogen in the presence of platinum oxide. *JACS,* **1930**, 52, 3010.

(25) Faba, L.; Díaz, E.; Ordóñez, S., Base-catalyzed condensation of levulinic acid: a new biorefinery upgrading approach. *ChemCatChem* **2016**, 8, 1490-1494. Doi: 10.1002/cctc/201600064.

(26) Amarasekara, A.S.; Ha, U.; Fonari, M.S.; Bejagam, S.N.; Margetic, D., Sulfuric acid and amberlyst-H+ catalyzed condensation reactions of renewable keto acids with paraformaldehyde: synthesis of a new dispiro bis-lactone ring system 2,9,13-trioxadispiro[4.1.4.3]tetradecane-3,6,10-trione. *RSC Adv*. **2017**, 7, 23917-23923. Doi: 10.1039/c7ra02303k.

(27) Li, Z.; Zhang, J.; Nielsen, M.M.; Wang, H.; Chen, C.; Xu, J.; Wang, Y.; Deng, T.; Hou, X., Efficient C-C bond formation between two levulinic acid molecules to produce C-10 compounds with the cooperation effect of Lewis and Bronsted acids. *ACS Sust. Chem. Eng*. **2018**, 6, 5708.5711. Doi: 10.1021/acssuschemeng.7b04621.

(28) Faba, L.; Díaz, E.; Ordóñez, S., Aqueous-phase furfural-acetone aldol condesnation over basic mixed oxides. *Appl. Catal. B* **2012**, 113-114, 201-211. Doi: 10.1016/j.apcatb.2011.11.039.

(29) Wang, W.; Li, N.; Li, G.; Li, S.; Wang, W.; Wang, A.; Cong, Y.; Wang, X.; Zhang, T., Synthesis of renewable high-density fuel with cyclopentanone derived from hemicellulose. *ACS Sust. Chem. Eng*. **2017**, 5, 1812-1817. Doi: 10.1021/ acssuschemeng.6b02554.

(30) Pagán-Torres, Y. J.; Wang, T.; Gallo, J. M. R.; Shanks, B. H.; Dumesic, J. A., Production of 5-hydroxymethylfurfural from glucose using a combination of Lewis and Brønsted acid catalysts in water in a biphasic reactor with an alkylphenol solvent. *ACS Catal.* **2012**, 2, 930-934. Doi: doi.org/10.1021/cs300192z.

(31) Bhanja, P.; Modak, A.; Chatterjee, S.; Bhaumik, A., Bifuncionalized mesoporous SBA-15: a new heterogeneous catalyst for the facile synthesis of 5-hydromethylfurfural. *ACS Sust. Chem. Eng*. **2017**, 5, 2763-2773. Doi: 10.1021/ acssuschemeng.6b03100.

(32) Garcés, D.; Faba, L.; Díaz, E.; Ordóñez, S., Aqueous-phase transformation of glucose into hydroxymethylfurfural and levulinic acid by combining homogeneous and heterogeneous catalysis. *ChemSusChem* **2019**, 12, 924-934. Doi: 10.1002/cssc.201802315.

(33) Huang, X.; Kudo, S.; Sperry, J.; Hayashi, J., Clean synthesis of 5- hydroxymethylfurfural and levulinic acid by aqueous Phase conversion of levoglucosenone over solid acid catalysts. *ACS Sust. Chem. Eng*. **2019**, 7, 5892-5899. oi: 10.1021/acssuschemeng.8b05873.

(34) Cueto, J.; Faba, L.; Díaz, E.; Ordóñez, S., Enhancement of furfural-cyclopentanone aldol condensation using binary water-ethanol mixtures as solvent. *J. Chem. Technol. Biotechnol.* **2018**, 93, 1563-1571. Doi: 10.1002/jctb.5522.

(35) Faba, L.; Díaz, E.; Ordóñez, S., Improvement on the catalytic performance of Mg-Zr mixed oxides for furfural-acetone aldol condensation by supporting on mesoporous carbons. *ChemSusChem* **2013**, 6, 463-473. Doi: 10.1002/cssc.201200710.

(36) Desai, D. S.; Yadav, G. D., Green synthesis of furfural acetone by solvent-free aldol condensation of furfural with acetone over La2O3-MgO mixed oxide catalyst. *ACS Sust. Chem. Eng*. **2019**, 58, 16096-16105. Doi: 10.1021/acssuschemeng.8b05873.

(37) Amarasekara, A.S.; Singh, T.B.; Larkin, E.; Hasan, M.A.; Fan, H.-J., NaOH catalyzed condensation reactions between levulinic acid and biomass derived furan-aldehydes in water. *Ind. Crops. Prod.* **2015**, 65, 546-549. Doi: 10.1016/j.indcrop.2014.10.005.

(38) Liang, G.; Wang, A.; Zhao, X.; Lei, N.; Zhang, T., Selective aldol condensation of biomass-derived levulinic acid and furfural in aqueous-phase over MgO and ZnO. *Green. Chem.* **2016**, 18, 3430-3438.

(39) Scanlon, J.T.; Willis, D.E., Calculation of flame ionization detector relative response factors using the effective carbon number concept. *J. Chromatogr. Sci.* **1985**, 23, 333-340. Doi: 10.1093/chromsci/23.8.333.

(40) De Melo Lima, T.; Weber Paixao, M.; Correa, A.G., Angelica lactones: from biomass-derived platform chemicals to value-added products. *ChemSusChem* **2018**, 11, 24-47. Doi: 10.1002/cssc.2017.01469.

(41) Che, Q.; Yang, M.; Wang, X.; Yang, Q.; Chen, Y.; Chen, X.; Chen, W.; Hu, J.; Zeng, K.; Yang, H.; Chen, H., Preparation of mesoporous ZSM-5 catalysts using green templates and their performance in biomass catalytic pyrolysis. *Bioresour. Technol.* **2019**, 289, 121729. Doi: 10.1016/j.biortech.2019.121729.

(42) Lok, C.M.; Van Doorn, J.; Almansa, G.A., Promoted ZSM-5 catalysts for the production of bio-aromatics, a review. *Renew. Sust. Energ. Rev.* **2019**, 113, 109248. Doi: 10.1016/j.rser.2019.109248.

(43) Kikhtyanin, O.; Kelbichová, V.; Vitvarová, D.; Kubu, M.; Kubicka, D., Aldol condensation of furfural and acetone on zeolites. *Catal. Today* **2014**, 227, 154-162. Doi: 10.1016/j.cattod.2013.10.059.

(44) Dumitriu, E.; Hulea, V.; Fechete, I.; Auroux, A.; Lacaze, J.-F.; Guimon, C., The aldol condensation of lower aldehydes over MFI zeolites with different acidic properties. *Micropor. Mesopor. Mater.* **2001**, 43, 341-359. Doi: 10.1016/S1387-1811(01)00265-7.

(45) Russo, V.; Hrobar, V.; Mäki-Arvela, P.; Eränen, K.; Sandelin, F.; Di Serio, M.; Salmi, T., Kinetics and modelling of levulinic acid esterficiation in batch and continuous reactors. *Top. Catal.* **2018**, 61, 1856-1865. Doi: 10.1007/s11244-018-0998-y.

(46) Jacobs, P.A.; Von Ballmoos, R., Framework hydroxyl groups of H-ZSM-5 zeolites. *J. Phys. Chem.* **1982**, 86, 3050-3052. Doi: 10.1021/j100212a046.

(47) Díez, V.K.; Apesteguía, C.R.; Di Cosimo J.I., Aldol condensation of citral with acetone on MgO and alkali-promoted MgO catalysts. *J. Catal*. **2006**, 240, 235-244. Doi: 10.1016/j.cat.2006.04.003.
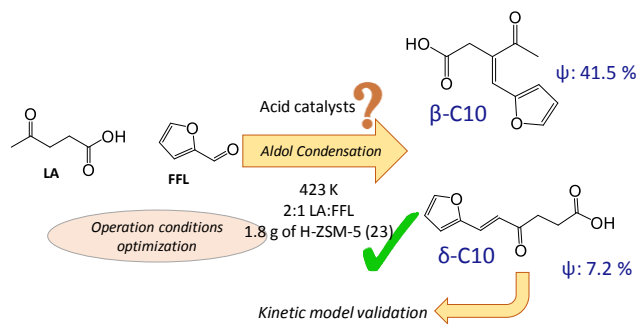
Acid-catalyzed condensation of furfural and levulinic acid is an attractive alternative for

obtaining renewable C10 chemicals at mild conditions.